



Fractal Structure of Seismic Signals of 2015 Gorkha-Kodari Earthquakes: A Box Counting Method

Ram Krishna Tiwari ^{1,2} Harihar Paudyal ²

¹ Central Department of Physics, Tribhuvan University, Kirtipur, Kathmandu, Nepal

² Department of Physics, Birendra Multiple Campus, Tribhuvan University, Bharatpur, Chitwan, Nepal

*Corresponding Author: ram.tiwari@bimc.tu.edu.np

Received: Aug. 12, 2022, Accepted: Nov. 30, 2022

Abstract

Fractal dimension analysis is a computational image processing technique that allows assessing the degree of complexity in patterns. In seismology, fractal dimensions can be used to describe fractured surfaces quantitatively. The larger the fractal dimension the more rugged is the surface, the more irregular is the line, and the more complex is the pore space. For the present investigation the seismic wave signal of 40 earthquakes including one foreshock, main shock and 38 aftershocks ($m_b \geq 5.0$) of 2015 Gorkha-Kodari earthquakes from 2015/4/21 to 2016/11/27 were considered. The seismograms were retrieved from the archived waveform data of Incorporated Research Institutions of Seismology (IRIS). The fractal dimension (D) was evaluated by the Python program for box counting. It is found that the fractal dimensions of the seismic wave signal during the active seismic period do not show sudden variation and they are almost identical. The maximum value was noticed to be 1.99 ± 0.006 and the minimum value to be 1.95 ± 0.007 . The estimated fractal dimension is greater or equal to 1.95 with an average value of 1.98 which signify the presence of high grade of fractality in seismic wave time series. This suggests that the fractal characteristics of the seismic wave signal of 2015 central Himalayan earthquakes occurrence behavior is nonlinear and coplanar.

Keywords Fractal dimension, Nonlinearity, Central Himalaya, Seismic wave signal

1. Introduction

The Himalayan arc between the Indian plate and the Eurasian plate had hosted many devastating earthquakes in the past. Recently on 25th of April 2015, the region was visited by another devastating earthquake known as Gorkha earthquake (Elliott et al., 2016; Gualandi et al., 2017; He et al., 2018). The main shock of magnitude 7.8 Mw (6.9 mb) hit nearly 80 km N-NE of Kathmandu in central Nepal and the event was followed by thousands of moderate to strong aftershocks (Yamada et al., 2020). A strong aftershock magnitude 6.5 mb occurred on the same day just after the 34 minutes of the main shock. Moreover, on April 26, another strong aftershock of magnitude 6.6 mb struck the region, and the strongest aftershock Mw 7.3 (6.7 mb) of the Gorkha seismic sequence was recorded on May 12, in the Kodari region, north-east of Kathmandu (Adhikari et al., 2015; Baillard et al., 2017). The three-dimensional visualization of earthquakes is depicted in figure1 showing the clustered seismicity around longitude 85°E to 87°E.

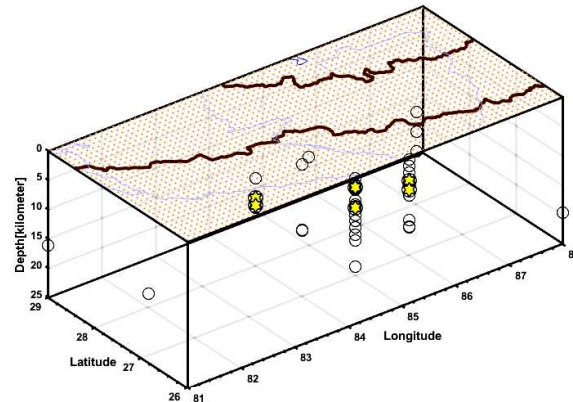


Fig. 1: Three-dimensional visualization of events where circles represent the earthquakes between magnitude 5.0 mb and less than 5.8 mb while yellow hexagams stand for the earthquake with magnitude ≥ 5.8 mb

Euclidean geometry or plane geometry is capable enough to describe regular structures. In Euclidean geometry, objects are solid and continuous, and they do not have holes or gaps. The dimensions of such objects are integers. It can be normally described by size of length, area, and volume. More importantly, the Euclidean dimension or embedding dimension is always an integer. It is 0 for point, 1 for line, 2 for surface, and 3 for volume and so on. Both a smooth line and a very wiggly line have same dimension 1 according to Euclidean geometry. In real sense, wiggly line could indeed fill up more space than a smooth line and it is the fractal object. It has complex geometry and shows the different length, area, and volume with changes with the scales. Their understandings require a meaning of dimension beyond the idea of conventional approach of dimension we learnt so far. Fractals are rough or discontinuous so they have fractional or fractal dimensions. The idea of fractal dimension had been introduced by Mandelbrot (Mandelbrot, 1967) and it can be applied to determine the self-similarity of the objects (Eke et al., 2002; Kurths et al., 2008). It has been used to identify the patterns in surface electromyography (EMG) signal (Hu et al., 2005). The fractal geometry has ability to express the irregular or fragmented shape of natural features and other complex objects whenever Euclidean geometry fails to analyze (Mandelbrot, 2003, 1989; Márquez-Rámirez et al., 2012).

The measurement of the fractal dimension of complex objects was popularized in many scientific fields, especially to time series in physics, engineering, and neurophysiology (Lopes & Betrouni, 2009; Telesca et al., 2015). Seismic wave signals are fractal time series data, and the fractal dimensionality associated with them contains information about the geometrical structure of the source (Maragos & Sun, 1993). In the past studies, the time interval between successive earthquakes of seismically active areas of central Italy was studied by using the Multifractal Detrended Fluctuation Analysis (MF-DFA) (Telesca et al., 2005). In the recent study of the earthquake distribution in the central Himalayan region, high box counting fractal dimension values (≥ 1.74) were

obtained indicating the near planar structure of the source zones (Tiwari & Paudyal, 2021). This paper is aimed at recognizing dissimilar patterns of seismic wave signals of 2015 Gorkha earthquake sequences according to box counting fractal dimension.

2. Data and methodology

We have retrieved the earthquake data from the catalogue of Internal Seismological Centre (ISC) considered 40 earthquakes (≥ 5 mb) including one foreshock, mainshock and aftershocks from April 2015 to November 2016 (2015/4/21–2016/11/27). The seismic wave signals for corresponding events were retrieved from Incorporated Research Institutions in Seismology (IRIS) for a period of two minutes i.e., one minute before and one minute after the event time mentioned in Table 1. We have used network AV, station RSO and channel EHZ for retrieving the signal from ObsPy (A Python Toolbox for Seismology) (Beyreuther et al., 2010). The instrument response of each seismic signal is removed before calculating the fractal dimension. In box counting method, the seismic signal is covered with a grid and numbers of boxes of the grid covering part of the signal are counted. By repeating the procedure with a finer grid having smaller boxes, the fractal dimension of the signal is estimated. The signals retrieved were depicted in figure 2.

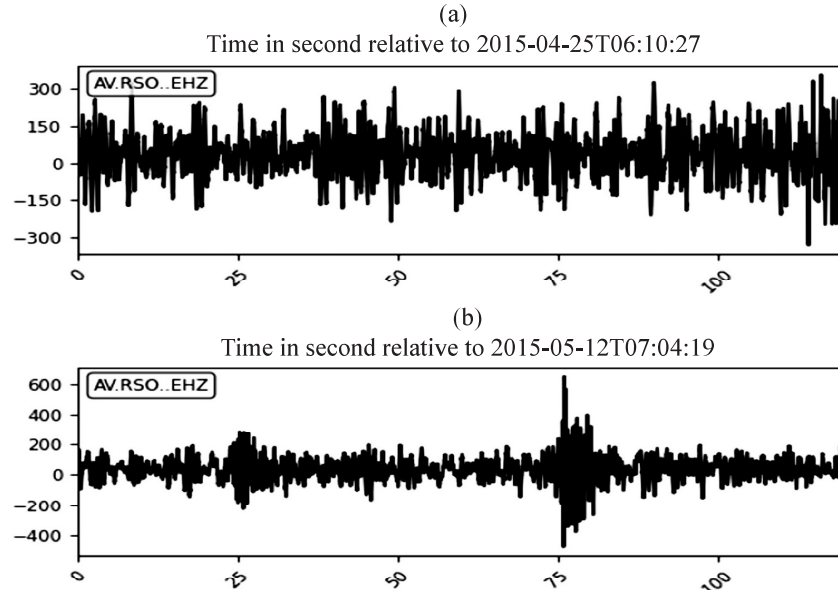


Fig. 2: Displacement time series of seismic wave signals of (a) main shock (7.8Mw) and (b) major aftershock (7.3 Mw)

2.1 Fractal dimension calculation

For the straight line divided into N equal parts to cover the line, each part has a size

$$r(N) = \frac{1}{N} \quad (1)$$

But to cover the rectangle there is a need for N^2 equal parts and size of single part

$$r(N) = \frac{1}{N^2} \tag{2}$$

For the parallelepiped

$$r(N) = \frac{1}{N^3} \tag{3}$$

Generalizing the results, we get

$$r(N) = \frac{1}{N^D} = N^{-\frac{1}{D}} \tag{4}$$

Where D is the dimension of the objects having non integer or fractional values.

2.2 Box counting dimensions

The generalization of box counting dimension is named after the German mathematician, Felix Hausdorff (Górski, 2001). The method is useful for both describing natural objects and for evaluating trajectories of dynamic systems as well. In box counting algorithm (Grassberger, 1983), a planar set S is enclosed with square boxes of size r and the number of square boxes required to cover S is counted (Gonzato, 1998). For the limiting value of r ($r \rightarrow 0$), the total area covered with square boxes will converge to the measure of S. It can be expressed mathematically by the relation

$$D = -\lim_{r \rightarrow 0} \frac{\log(n_r(S))}{\log\left(\frac{1}{r}\right)}$$

The fractal dimension (D) is estimated from the slope of straight line obtained from a plot of $\log n_r(S)$ versus $\log r$ (Figure 3).

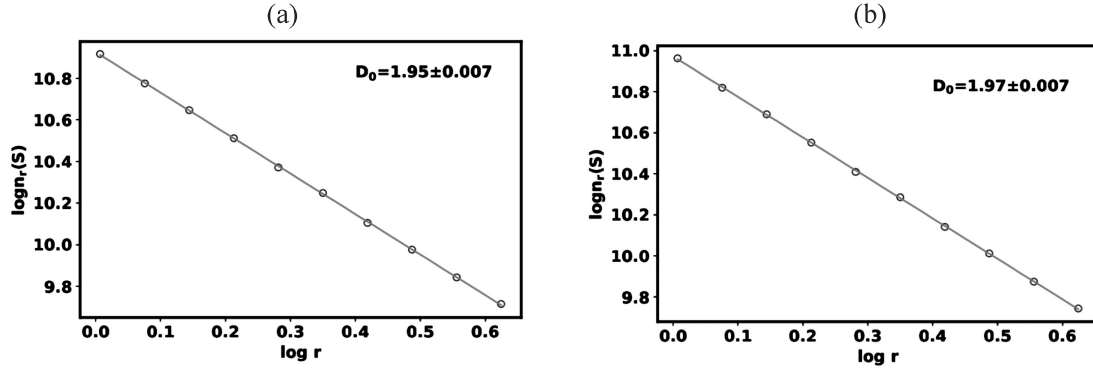


Fig. 3: The estimation of fractal dimension of (a) main shock (7.8Mw) and (b) major aftershock (7.3 Mw)

3. Results and discussion

The fractal dimensions of seismic signal corresponding to each earthquake are computed and presented in table 1. As an example of the dimension calculation procedure, the log-log plots for main shock (Gorkha earthquake) and major after shock (Kodari earthquake) are depicted in figure 3. The fractal dimension of main shock (6.9 mb) signal and 6.5 mb aftershock signal on the same day were found to be 1.95 ± 0.007 and 1.98 ± 0.007 , respectively. The fractal dimension is 1.98 ± 0.006 for 6.6 mb aftershock

signal that recorded day after the main event. The fractal dimension (1.97 ± 0.007) for 6.7 mb major aftershock signal on 2015/5/12 is similar to the fractal dimension of 6.1 mb aftershock signal on the same day. We noticed the small variation of fractal dimension from 1.95 ± 0.007 to 1.99 ± 0.006 for all considered seismic wave time series. The estimated fractal dimension is greater or equal to 1.95 with an average value of 1.98. This result assures the presence of a high degree of fractality in the signals. The preceding study also noticed the increase in multifractality of the seismic wave signals of 2015 Gorkha earthquake and its aftershock (Tiwari et al., 2020). A sudden drop of fractal dimension for electromagnetic emission prior to significant earthquake (Lu et al., 2005; Potirakis et al., 2012) and in laboratory experiments (Kapiris et al., 2005) are noticed, however we did not notice such type of variation in the seismic wave time series of Gorkha-Kodari earthquakes.

Table 1: Earthquake events with date of occurrence, time of occurrence, latitude, longitude, depth, magnitude and box counting fractal dimension

S N	Date	time	latitude	longitude	Depth (km)	Magnitude (mb)	Fractal dimension (D)
1	4/21/2015	14:02:17	28.8557	82.359	22.7	5.0	1.98±0.007
2	4/25/2015	06:11:27	28.1302	84.7168	13.4	6.9	1.95±0.007
3	4/25/2015	06:15:23	27.6342	85.4762	10.0	6.1	1.98±0.007
4	4/25/2015	06:18:00	27.7097	85.9014	10.0	5.3	1.96±0.006
5	4/25/2015	06:18:13	27.6955	85.9601	19.0	5.6	1.97±0.006
6	4/25/2015	06:20:40	28.202	84.6237	10.0	5.3	1.98±0.006
7	4/25/2015	06:22:03	27.7884	85.1449	12.1	5.1	1.99±0.006
8	4/25/2015	06:22:23	27.8287	85.455	18.0	5.0	1.99±0.006
9	4/25/2015	06:25:56	27.699	85.5783	15.6	5.0	1.99±0.006
10	4/25/2015	06:37:59	27.8009	85.8073	14.7	5.1	1.98±0.007
11	4/25/2015	06:45:21	28.1603	84.8433	14.7	6.5	1.98±0.006
12	4/25/2015	06:56:34	27.8635	85.7138	8.4	5.5	1.99±0.006
13	4/25/2015	06:58:28	27.7032	85.9789	13.3	5.1	1.99±0.006
14	4/25/2015	07:47:02	27.8734	85.5984	10.1	5.0	1.98±0.007
15	4/25/2015	08:55:56	27.5796	85.5542	12.9	5.2	1.98±0.006
16	4/25/2015	09:17:02	28.3483	87.2873	9.3	5.6	1.98±0.006
17	4/25/2015	12:44:06	28.0803	84.6417	15.1	5.1	1.97±0.006
18	4/25/2015	17:42:52	28.2579	85.8625	9.9	5.3	1.97±0.007
19	4/25/2015	23:16:15	27.7744	84.9497	13.7	5.5	1.96±0.007
20	4/26/2015	07:09:09	27.7365	85.9788	13.4	6.6	1.98±0.006
21	4/26/2015	16:26:06	27.7996	85.8233	16.8	5.6	1.97±0.007
22	4/27/2015	12:35:52	26.8348	88.0797	19.6	5.2	1.99±0.006
23	5/12/2015	07:05:19	27.8014	86.126	12.3	6.7	1.97±0.007
24	5/12/2015	07:17:21	27.7251	86.2083	12.6	5.4	1.99±0.006
25	5/12/2015	07:23:33	27.3792	86.2416	19.0	5.0	1.99±0.006
26	5/12/2015	07:34:23	27.6932	86.2267	11.0	5.3	1.97±0.006

27	5/12/2015	07:36:53	27.5248	86.1418	13.8	6.1	1.97±0.007
28	5/12/2015	08:06:08	27.669	86.088	20.3	5.1	1.98±0.007
29	5/12/2015	08:13:54	27.7404	85.8442	9.5	5.1	1.97±0.006
30	5/12/2015	08:21:10	27.6801	86.1084	9.8	5.2	1.96±0.007
31	5/12/2015	21:25:11	27.7651	84.7136	2.5	5.1	1.98±0.006
32	5/16/2015	11:34:11	27.5175	86.1127	20.1	5.6	1.98±0.006
33	8/23/2015	09:02:04	27.7509	86.0641	8.7	5.1	1.97±0.007
34	11/19/2015	04:15:52	27.7947	85.6871	10.4	5.0	1.97±0.006
35	12/18/2015	22:16:56	29.2787	81.6399	16.1	5.3	1.98±0.006
36	2/5/2016	16:20:11	27.8644	85.457	23.4	5.2	1.97±0.007
37	2/21/2016	18:10:00	27.9582	84.717	13.8	5.0	1.97±0.006
38	5/22/2016	01:48:49	28.3812	87.5079	16.0	5.0	1.98±0.007
39	5/22/2016	02:05:55	28.4487	87.428	12.7	5.1	1.98±0.006
40	11/27/2016	23:35:21	27.7097	86.5045	14.8	5.4	1.98±0.007

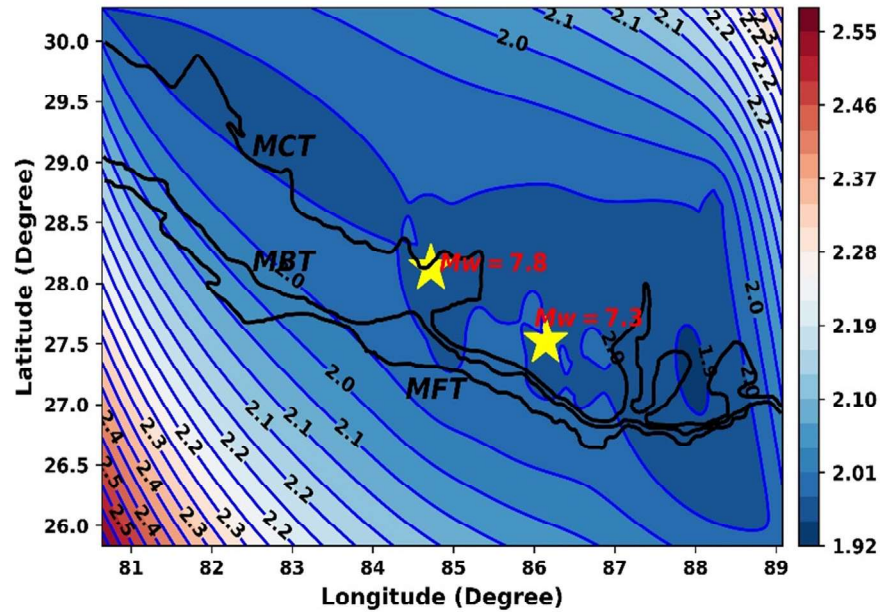


Fig. 4: Contour map of fractal dimension value for the study region where MCT, MBT, and MFT are abbreviations for Main Central Thrust, Main Boundary Thrust, and Main Frontal Thrust, respectively. Two yellow stars stand for the Gorkha earthquake and Kodari earthquake of 2015.

The fractal dimension contour map is depicted in figure 4. The high D value contour lines show that the region is dominated by fractal dimension values between 1.92 to around 2.0. These high values of dimension may be associated with different underlying geometrical structures and different dynamics operating in the region.

4. Conclusion

Fractal objects have non-integer fractional dimension rather than an integer Euclidean dimensionality. All fractal objects exhibit self-similar or self-affine character (exact or statistical); this means that objects look the same at different levels of magnification (Narine & Marangoni, 1999). Fractal geometry has been reported to characterize brittle deformation structures in the crust over several bands of length scales, from regional fault networks through main traces of individual faults to the internal structure of fault zones. Another characteristic of fractal objects is that a specific property should scale in a power-law fashion within a length scale. It has for long been suggested that fractured rock surfaces are fractals. The fractal geometry implies a balance between two competing processes: strain weakening and strain hardening. This balance is critically tuned to produce neither positive nor negative feedback mechanisms during deformation. In such a case, the long-term deformation is accommodated statistically, at all-time intervals, by structures that have no preferred size scale, i.e., structures following a scale free frequency-size distribution. In fact, fault surfaces are fractals can be interpreted as the fractal dimension of the fault system. The application of nonlinear science has been used to find the fractal dimension of the seismic signals recorded at IRIS. Seismic wave signals before and after the Gorkha earthquake have been analyzed in terms of box counting fractal dimension. The results show almost identical value of the fractal dimension for active seismic period. The fractal dimensions of seismic wave signal do not show significant variation during the time of the active seismic period. Thus, time series seismic signals are complex and have fractal characteristics that exists self-similarity phenomenon, i.e., pieces of a fractal object are similar to that of the whole implying fractal models of earthquake dynamics.

Acknowledgments

One of the author (RKT) would like to express acknowledgement to Tribhuvan University, Nepal for providing the sabbatical leave and to the University Grants Commission, Nepal for providing the financial support under the PhD grant S&T -14-075/76. The authors would also like to thank the reviewers for their suggestions and comments to improve the quality of this manuscript.

References

- Adhikari, L. B., Gautam, U. P., Koirala, B. P., Bhattarai, M., Kandel, T., Gupta, R. M., Timsina, C., Maharjan, N., Maharjan, K., Dahal, T., Hoste-Colomer, R., Cano, Y., Dandine, M., Guilhem, A., Merrer, S., Roudil, P., & Bollinger, L. (2015). The aftershock sequence of the 2015 april 25 Gorkha-Nepal earthquake. *Geophysical Journal International*, 203(3), 2119–2124. <https://doi.org/10.1093/gji/ggv412>
- Baillard, C., Lyon-Caen, H., Bollinger, L., Rietbrock, A., Letort, J., & Adhikari, L. B. (2017). Automatic analysis of the Gorkha earthquake aftershock sequence: Evidences of structurally segmented seismicity. *Geophysical Journal International*, 209(2), 1111–1125. <https://doi.org/10.1093/gji/ggx081>

- Beyreuther, M., Barsch, R., Krischer, L., Megies, T., Behr, Y., & Wassermann, J. (2010). ObsPy: A Python Toolbox for Seismology. *Seismological Research Letters*, 81(3), 530–533. <https://doi.org/https://doi.org/10.1785/gssrl.81.3.530>
- Eke, A., Herman, P., Kocsis, L., & Kozak, L. R. (2002). Fractal characterization of complexity in temporal physiological signals. *Physiological Measurement*, 23(1). <https://doi.org/10.1088/0967-3334/23/1/201>
- Elliott, J. R., Jolivet, R., Gonzalez, P. J., Avouac, J. P., Hollingsworth, J., Searle, M. P., & Stevens, V. L. (2016). Himalayan megathrust geometry and relation to topography revealed by the Gorkha earthquake. *Nature Geoscience*, 9(2), 174–180. <https://doi.org/10.1038/ngeo2623>
- Gonzato, G. (1998). A practical implementation of the box counting algorithm. *Computers and Geosciences*, 24(1), 95–100. [https://doi.org/10.1016/S0098-3004\(97\)00137-4](https://doi.org/10.1016/S0098-3004(97)00137-4)
- Górski, A. Z. (2001). Pseudofractals and the box counting algorithm. *Journal of Physics A: Mathematical and General*, 34(39), 7933–7940. <https://doi.org/10.1088/0305-4470/34/39/302>
- Grassberger, P. (1983). Generalized dimensions of strange attractors. *Physics Letters A*, 97(6), 227–230. [https://doi.org/10.1016/0375-9601\(83\)90753-3](https://doi.org/10.1016/0375-9601(83)90753-3)
- Gualandi, A., Avouac, J. P., Galetzka, J., Genrich, J. F., Blewitt, G., Adhikari, L. B., Koirala, B. P., Gupta, R., Upreti, B. N., Pratt-Sitaula, B., & Liu-Zeng, J. (2017). Pre- and post-seismic deformation related to the 2015, Mw7.8 Gorkha earthquake, Nepal. *Tectonophysics*, 714–715, 90–106. <https://doi.org/10.1016/j.tecto.2016.06.014>
- He, P., Lei, J., Yuan, X., Xu, X., Xu, Q., Liu, Z., Mi, Q., & Zhou, L. (2018). Lateral Moho variations and the geometry of the Main Himalayan Thrust beneath the Nepal Himalayan orogen revealed by teleseismic receiver functions. *Geophysical Journal International*, 214(2), 1004–1017. <https://doi.org/10.1093/gji/ggy192>
- Hu, X., Wang, Z. Z., & Ren, X. M. (2005). Classification of surface EMG signal with fractal dimension. *Journal of Zhejiang University: Science*, 6 B(8), 844–848. <https://doi.org/10.1631/jzus.2005.B0844>
- Kapiris, P., Nomicos, K., Antonopoulos, G., Polygiannakis, J., Karamanos, K., Kopanas, J., Zissos, A., Peratzakis, A., & Eftaxias, K. (2005). Distinguished seismological and electromagnetic features of the impending global failure: Did the 7/9/1999 M5.9 Athens earthquake come with a warning? *Earth, Planets and Space*, 57(3), 215–230. <https://doi.org/10.1186/BF03351818>
- Kurths, J., Schwarz, U., Witt, A., Krampe, R. T., & Abel, M. (1996, June). *Measures of complexity in signal analysis*. In AIP Conference Proceedings (Vol. 375, No. 1, PP.(33-54). American Institute of Physics.
- Lopes, R., & Betrouni, N. (2009). Fractal and multifractal analysis: A review. *Medical Image Analysis*, 13(4), 634–649. <https://doi.org/10.1016/j.media.2009.05.003>
- Lu, C., Mai, Y.-W., & Xie, H. (2005). A sudden drop of fractal dimension: a likely precursor of catastrophic failure in disordered media. *Philosophical Magazine Letters*, 85(1), 33–40. <https://doi.org/https://doi.org/10.1080/09500830500153883>

- Mandelbrot, B. (1967). How long is the coast of Britain? Statistical self-similarity and fractional dimension. *Science*, 156(3775), 636–638. <https://doi.org/10.1126/science.156.3775.636>
- Mandelbrot, B. B. (2003). Multifractal Power Law Distributions: Negative and Critical Dimensions and Other “Anomalies,” Explained by a Simple Example. *Journal of Statistical Physics*, 110(3–6), 739–774. <https://doi.org/10.1023/A:1022159802564>
- Mandelbrot, B. B. (1989). Multifractal Measures, Especially for the Geophysicist. *Pure and Applied Geophysics*, 131(1/2).
- Maragos, P., & Sun, F. K. (1993). Measuring the Fractal Dimension of Signals: Morphological Covers and Iterative Optimization. *IEEE Transactions on Signal Processing*, 41(1), 108. <https://doi.org/10.1109/TSP.1993.193131>
- Márquez-Rámirez, V. H., Pichardo, F. A. N., & Reyes-Dávila, G. (2012). Multifractality in Seismicity Spatial Distributions: Significance and Possible Precursory Applications as Found for Two Cases in Different Tectonic Environments. *Pure and Applied Geophysics*, 169(12), 2091–2105. <https://doi.org/10.1007/s00024-012-0473-9>
- Narine, S. S., & Marangoni, A. G. (1999). Fractal nature of fat crystal networks. *Physical Review E*, 59(2), 1908–1920. <https://doi.org/10.1103/physreve.59.1908>
- Potirakis, S. M., Minadakis, G., & Eftaxias, K. (2012). Sudden drop of fractal dimension of electromagnetic emissions recorded prior to significant earthquake. *Natural Hazards*, 64(1), 641–650. <https://doi.org/doi:10.1007/s11069-012-0262-x>
- Telesca, L., Lapenna, V., & MacChiato, M. (2005). Multifractal fluctuations in seismic interspike series. *Physica A: Statistical Mechanics and Its Applications*, 354(1–4), 629–640. <https://doi.org/10.1016/j.physa.2005.02.053>
- Telesca, L., Lovallo, M., Martí Molist, J., López Moreno, C., & Abella Meléndez, R. (2015). Multifractal investigation of continuous seismic signal recorded at El Hierro volcano (Canary Islands) during the 2011–2012 pre- and eruptive phases. *Tectonophysics*, 642(1), 71–77. <https://doi.org/10.1016/j.tecto.2014.12.019>
- Tiwari, B. R., Xu, J., Adhikari, B., & Chapagain, N. P. (2020). Multifractal analysis for seismic wave in Kathmandu valley after Gorkha Earthquake-2015, Nepal. *Journal of Nepal Physical Society*, 6(2), 113–120. <https://doi.org/10.3126/jnphysoc.v6i2.34866>
- Tiwari, R. K., & Paudyal, H. (2021). Box counting fractal dimension and frequency size distribution of earthquakes in the central Himalaya region. *Journal of Institute of Science and Technology*, 26(2), 127–136. <https://doi.org/https://doi.org/10.3126/jist.v26i2.41664>
- Yamada, M., Kandel, T., Tamaribuchi, K., & Ghosh, A. (2020). 3D fault structure inferred from a refined aftershock catalog for the 2015 gorkha earthquake in Nepal. *Bulletin of the Seismological Society of America*, 110(1), 26–37. <https://doi.org/10.1785/0120190075>